Chemical Science

Accepted Manuscript

Chemical Science

rsc.li/chemical-science

Volume 9
Number 1
7 January 2018
Pages 1-268

ISSN 2041-6539

ROYAL SOCIETY OF CHEMISTRY

EDGE ARTICLE
Xinjing Tang et al.
Caged circular siRNAs for photomodulation of gene
expression in cells and mice

ROYAL SOCIETY OF CHEMISTRY

rsc.li/chemical-science

ARTICLE

Scale-Up of Microdroplet Reactions by Heated Ultrasonic Nebulization

Chengyuan Liu[a, ‡], Jia Li[a, ‡], Hao Chen[b], Richard N. Zare[a,*]

Dramatically higher rates for a variety of chemical reactions have been reported in microdroplets compared with those in the liquid bulk phase. However, the scale-up of microdroplet chemical synthesis has remained a major challenge to the practical application of microdroplet chemistry. Heated ultrasonic nebulization (HUN) was found as a new way for scaling up chemical synthesis in microdroplets. Four reactions were examined, a base-catalyzed Claisen–Schmidt condensation, an oximation reaction from a ketone, a two-phase oxidation reaction without the use of phase-transfer-catalyst, and an Eschenmoser coupling reaction. These reactions show one to three orders of magnitude of acceleration (122, 23, 6536, and 62) in HUN microdroplets compared to the same reactions in bulk solution. Then, using the present method, scale-up of the reactions was achieved at an isolated rate of 19 mg min^{-1} for the product of the Claisen–Schmidt condensation, 21 mg min^{-1} for the synthesis of benzophenone oxime from benzophenone, 31 mg min^{-1} for the synthesis of 4-methoxybenzaldehyde from 4-methoxybenzyl alcohol, and 40 mg min^{-1} for the enaminone product of the Eschenmoser coupling reaction.

Introduction

A number of recent studies[1-11], including work of our own,[12-16] have reported the acceleration of reaction rates in microdroplets formed in the course of spray-based ionization[4, 13, 17] and microfluidics.[18, 19] Microdroplets show a strikingly different reactive environment from that of the corresponding bulk phase.[5, 18, 20] The alteration of pH[21], the accumulation of reagents[5] on the microdroplet surface, solvent evaporation, confinement of reagents, and the high surface-to-volume ratio of the microdroplet are thought to contribute to the reaction acceleration.[1] The acceleration phenomena in confined volumes have also been reported in Leidenfrost levitated droplets[22] and thin films.[23, 24] The applicability of microdroplets in organic chemical synthesis is attracting increasing attention because in addition to reaction rate acceleration, sometimes microdroplet reactions can also proceed well without the use of a catalyst.[12, 16]

The droplets in microfluidic channels can be used as chemical microreactors for performing many reactions on a small scale.[25-28] Thus droplet-based microfluidics has been widely used for the high-throughput screening of diverse chemical and biochemical reactions.[29-32] Preparative organic synthesis in microemulsions can be facilitated by continuous-flow microfluidic devices.[33-36] Recently, many organic reactions[1, 3, 4, 6, 13, 14, 37-40] have been demonstrated to occur on the millisecond timescale in microdroplet reactions in air generated in electrospray ionization mass spectrometry (ESI-MS). However, the flow rate (ca. 10 µL/min) for microdroplet reaction in ESI-MS is not high enough for preparative organic synthesis. Although multiplexed ESI sprayer tips[3, 16] have even been used as a preparative method, the scale-up of microdroplet reactions in air is still challenging.

Ultrasonic nebulization (UN), i.e., the emission of a fog of microdroplets from an acoustically excited liquid–air interface, has been well-known since the landmark work report by Wood and Loomis in 1927.[41] Since then, UN has been used commercially in air humidifiers, medical nebulizers, and other such devices. UN has also been used as a method of sample atomization for subsequent ionization such as inductively coupled plasma,[42, 43] electrospray ionization (ESI),[44, 45] extractive electrospray ionization,[46] and photoionization[47, 48] in MS. Ultrasonically generated microdroplets have also been used as microreactors for the synthesis of semiconductor nanoparticles,[49] porous carbon powders,[50] and other nanostructured materials.[51] Ambient ionization MS was even applied for the real-time monitoring of microreactions in acoustically levitated droplets for which at least an order of magnitude faster reaction rate was observed.[52] Herein, we demonstrate the use of heated, UN-generated microdroplets (HUN) to perform the scale-up of four different chemical syntheses.

Figure 1 presents the experimental design for HUN microdroplet synthesis. When the ultrasonic nebulizer (Model 402AI, Yuwell Medical Equipment & Supply Corp., Suzhou, China) is switched on, the reactant solution in the nebulization cell can be continuously atomized into large amounts of

[a.] Dr. C.Y. Liu, J. Li, Prof. R. N. Zare
Department of Chemistry, Fudan University, Shanghai 200438, China Email: rnz@fudan.edu.cn
[b.] Prof. H. Chen
Department of Chemistry & Environmental Science, New Jersey Institute of Technology, Newark, NJ 07102, USA
‡ C.Y. Liu and J. Li contributed equally to this work.

microdroplets due to the so-called "ultrasonic fountain". Compared with the traditional ESI sprayer, the HUN setup enabled the reuse of reactant solution for microdroplet reaction. The working frequency of the transducer of the ultrasonic nebulizer is 1.7 MHz ± 10 %. The glass nebulization cell consists of a cylindrical upper part (I.D. 35 mm, height 90 mm) and lower part (I.D. 22 mm, height 15 mm). A thin polyethylene membrane transparent to ultrasonic waves, which is fixed by nylon cable ties, covers the bottom of the nebulization cell. Water between the polyethylene membrane and the transducer transfers the ultrasonic waves. In addition, a temperature-controlled heating tape (ZhengLong Electrothermal Technology Co., Ltd., China) is wound around the nebulization cell to assist in the microdroplet reaction. For comparison, all the bulk reactions were conducted at the same temperature. In the present design, no electric potential is applied but for some cases charging the microdroplets can be advantageous.
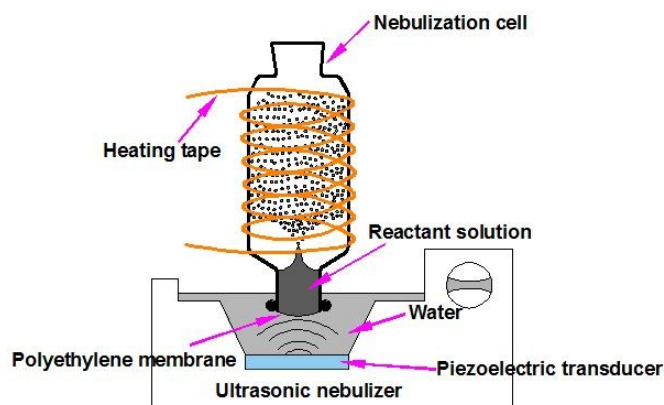

Figure 1. The heated ultrasonic nebulization (HUN) system used to generate continuously microdroplets in which chemical reactions are accelerated.

Results and discussion

At first, the base-catalyzed Claisen-Schmidt condensation between 6-hydroxy-1-indanone **1** and benzaldehyde **2** was investigated as a model reaction (See Figure 2). The acceleration of a similar system has been well-characterized by paper spray,[23, 53] ESI,[3] thin film,[24] and the Leidenfrost droplet reaction.[22] A recent study reported that moderate heat can accelerate the solvent evaporation from microdroplets and improve the reaction rate of the ESI microdroplet reaction.[54] The influence of temperature on the microdroplet reaction in the HUN system was investigated at first. As shown in Figure S1, temperature is quite an important factor, and the ratio of the MS product (6-hydroxy-2-benzyliden-1-indanone **3**) signal at m/z 235 to the reagent (6-hydroxy-1-indanone **1**) signal at m/z 147 increased markedly with elevation of the temperature from 30 °C to 50 °C. However, when increasing further the heating from 50 °C to 60 °C, no higher signal intensity of product **3** was observed and byproducts emerged. Thus, 50 °C was selected as the heating temperature for HUN microdroplet reactions, and the same temperature was used for the control experiments in bulk phase. The effect of temperature for this reaction in bulk phase was also

investigated. As presented in Figure S3, the ratio of product **3** and reactant **1** increased only twofold when the temperature was increased from 30 °C to 50 °C in bulk phase. Compared with bulk phase, the increased temperature in HUN can decrease the size of microdroplets, which was measured by a laser diffractometer (Sympatec HELOS, Sympatec, Germany). The experimental setup and results were shown in Figure S3. As the temperature was increased from 30 °C to 50 °C, the average droplet size was decreased from 6.9 μm to 5.4 μm, which is closer to the microdroplet size (2-3 μm) in ESI. Previous reports[39, 55, 56] have indicated that the droplet size has a large effect on the reaction rate in microdroplets; thus we speculate that the increased reaction rate in HUN at higher temperature is caused by the smaller droplet size. The following three reactions were also conducted at 50 °C. The reaction in the nebulization cell is accelerated by the continuously atomized microdroplets from the reactant solution. The effect of reaction time on the yield of product **3** for the Claisen-Schmidt condensation reaction in HUN microdroplets was also examined (Figure S4). The ratio of product **3** and reactant **1** increased during the initial 120 s due to the recycling of the reactant solution and remained unchanged at longer reaction times (up to 300 s). The influence of the volume of reactant solution in nebulization cell on the conversion efficiency was also tested. As shown in Figure S5, as the volume was increased from 1.2 mL to 2.4 mL, the ratio of product **3** and reactant **1** gradually decreased. It is speculated that the greater probability of recombination of microdroplets resulted in the lower reaction rate and lower conversion efficiency when higher volume reactant solution was nebulized into larger amounts of microdroplets in the confined space of ultrasonic the nebulization cell.
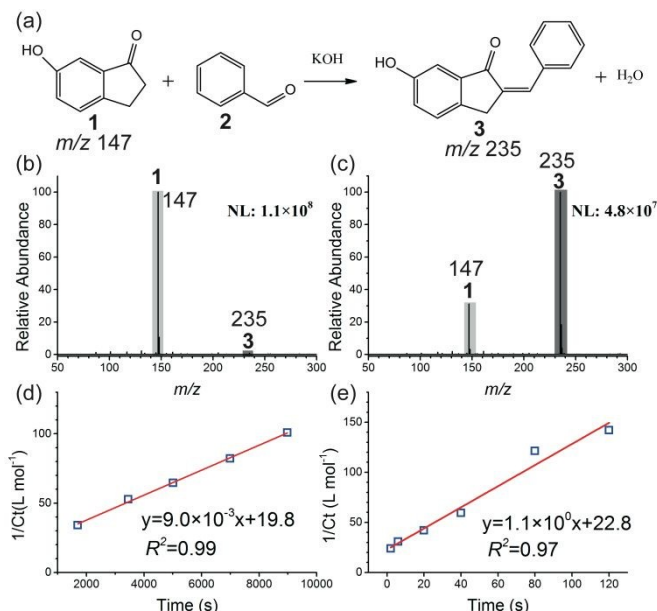
Figure 2. Base-catalyzed Claisen–Schmidt condensation of 6-hydroxy-1-indanone **1** with benzaldehyde **2** to form the product **3**: (a) reaction schematic; negative ion mode mass spectra of the condensation reaction in (b) bulk phase and (c) HUN microdroplets after 2 min. Plots of $1/C_t$ vs time for second-order reaction kinetics driving the reaction rate constant to be (d) 9.0×10^{-3} L mol^{-1} s^{-1} in bulk and (e) 1.1×10^{0} L mol^{-1} s^{-1} in HUN microdroplets.

Chemical Science Accepted Manuscript

According to MS peak intensities of the reactant **1** and product **3**, we can calculate the remaining concentration of reactant **1** (C_t) and yield of product **3** ($Y_{calculated}$). The reactant was found to ionize 2.2 times more efficiently than the product, resulting in a greater signal intensity for the same concentration of material (Figure S6). By monitoring the reaction with time, we calculated the reaction rate constants in bulk (k_{bulk}) and HUN microdroplets (k_{HUN}). The ratio between k_{HUN} and k_{bulk} gives the acceleration factor (AF). Section 4 of the Supporting Information describes the details of these calculations.

Figures 2b and 2c present the mass spectra of the condensation reaction in bulk phase and HUN microdroplets after 2 min. Compared to the 2-min yield in bulk phase (1.6%), a much higher 2-min yield (87.6%) can be obtained by the HUN microdroplet reaction. The reaction rate constants in bulk phase (k_{bulk}) and HUN microdroplets (k_{HUN}) at 50 °C were calculated by plotting the reciprocal of the remaining concentration of reactant **1** ($1/C_t$) against reaction time in Figures 2d and 2e. The HUN microdroplet reaction showed an acceleration factor of 122 over the bulk phase reaction. An industrial nebulization plate with 10 ultrasonic nebulizers (Figure S17) was used for the scale-up experiment, and 37.2 mg product was produced within 2 minutes (ca. 19 mg min⁻¹). Multiplexed ESI sprayer tips (25 µL/min per spray tip) have been used previously for the preparative synthesis of products from the Claisen-Schmidt condensation reaction in microdroplets, but only 0.588 mg min⁻¹ product was produced.[3] The highest yield for the preparative synthesis of the product of this condensation reaction in confined volume was ever achieved by a thin film, and only 98 mg h⁻¹ (ca. 1.6 mg min⁻¹) was reached.[24] Thus, HUN is a promising new method for the scale-up of microdroplet chemical synthesis. Table 1 lists the results for the condensation reaction.

The oximation reaction of benzophenone **4** with hydroxylamine **5** (Figure 3a) was also investigated to yield the corresponding benzophenone oxime **6**, which is an important reaction material for amide synthesis by the Beckman rearrangement reaction.[57] This reaction has previously been investigated using an ESI sprayer (10 µL/min) and showed a

significant rate acceleration.[58] However, the rate of product production obtained by the microdroplet reaction was too small (less than 50 µg min⁻¹).[58] Figures 3b and 3c show respectively the HPLC chromatograms of the oximation reaction in bulk phase and HUN microdroplets after 2 min. The concentration of hydroxylamine **5** in this experiment was maintained 20 times higher than that of benzophenone **4**; thus, the oximation reaction followed pseudo first-order kinetics. Figures 3d and 3e present plots of $\ln(C_t/C_0)$ vs time (C_t and C_0 represent the remaining and initial concentrations of reactant **4**) of this reaction in bulk phase and HUN microdroplets, respectively. As listed in Table 1, the reaction rate constant in HUN microdroplets (k_{HUN}) is 23-fold higher than that in bulk (k_{bulk}). For preparative synthesis, 41.5 mg benzophenone oxime was synthesised from benzophenone within 2 minutes (ca. 21 mg min⁻¹) by the setup shown in Figure S17.
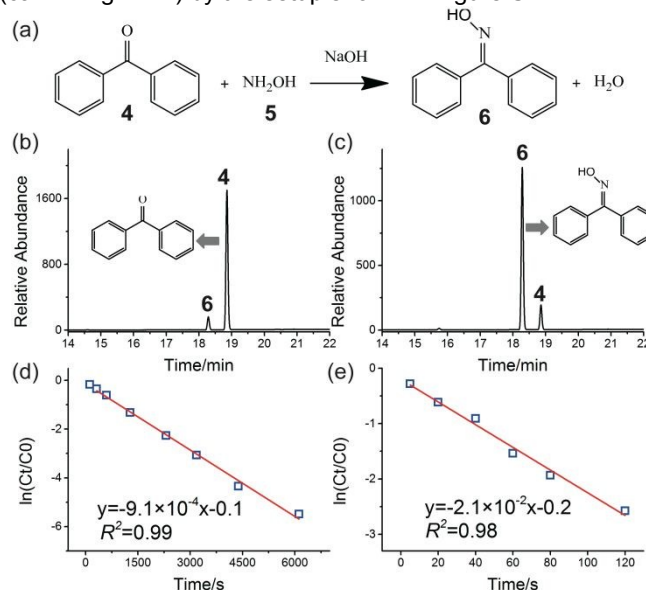
Figure 3. Oximation reaction of benzophenone **4** with hydroxylamine **5** to form benzophenone oxime **6**: (a) reaction schematic; HPLC chromatograms of oximation reaction in bulk phase (b) and HUN microdroplets (c) after 2 min. A higher yield of product **6** was obtained in HUN microdroplets. Plots of $\ln(C_t/C_0)$ vs time deriving the pseudo first-order reaction rate constant to be (d) 9.1×10^{-4} s⁻¹ in bulk and (e) 2.1×10^{-2} s⁻¹ in HUN microdroplets.

Table 1. Reaction rate constants (k_{bulk} and k_{HUN}) and acceleration factors (AF) for different reactions in bulk phase and HUN microdroplets. $Y_{calculated}$ is the calculated reaction yield based on MS and HPLC mesurements, and $Y_{isolated}$ is the isolated yield.

Reaction type	k_{bulk}	k_{HUN}	AF	$Y_{calculated}$	Isolated amount*	$Y_{isolated}$
Claisen–Schmidt condensation	9.0×10^{-3} L mol⁻¹ s⁻¹	1.1×10^{0} L mol⁻¹ s⁻¹	122	87.6%	37.2 mg	78.8%
Oximation reaction	9.1×10^{-4} s⁻¹	2.1×10^{-2} s⁻¹	23	92.4%	41.5 mg	84.3%
Two-phase reaction	1.1×10^{-6} s⁻¹	7.3×10^{-3} s⁻¹	6536	75.4%	93 mg	68.4%
Eschenmoser coupling reaction	1.4×10^{-3} L mol⁻¹ s⁻¹	8.7×10^{-2} L mol⁻¹ s⁻¹	62	78%	140 mg	67%

* The isolated amount is obtained by using 10 reactors based on an industrial nebulization plate. All the reactions were conducted at 50 °C. The reaction times for the Claisen-Schmidt condensation, the oximation reaction, the two-phase reaction and the Eschenmoser coupling reaction are 2 min, 2 min, 3 min and 3.5 min, respectively. The reactant solution volumes for the Claisen-Schmidt condensation, the oximation reaction, the two-phase reaction and the Eschenmoser coupling reaction are 1.2 mL, 1 mL, 1.1 mL, and 1 mL, respectively.

When a bulk liquid-liquid two-phase system is nebulized as small microdroplets, the interfacial area of the two-phases can be increased by many orders of magnitude. Thus, the two-

phase reaction was readily facilitated without the use of a phase-transfer-catalyst (PTC) in ESI microdroplets[16, 54], which meets the requirement of green chemistry and sustainable

synthesis. In this study, the two-phase reaction of 4-methoxybenzyl alcohol **7** in ethyl acetate (EtOAc) with aqueous NaClO (Figure 4a) was examined without using PTC.
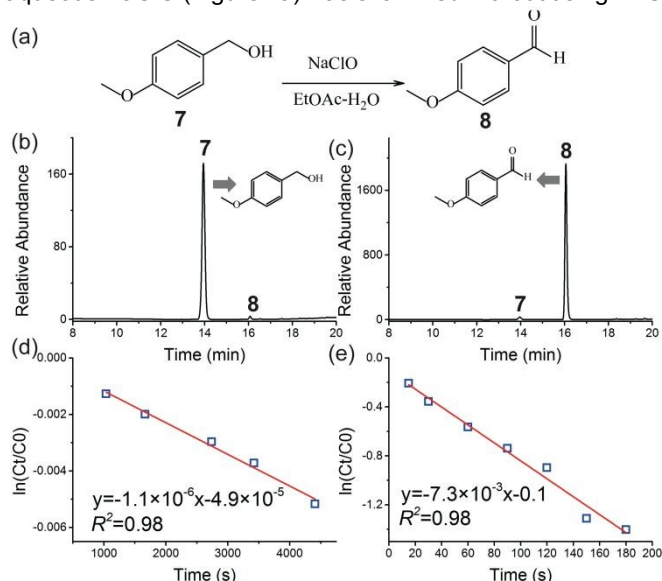

Figure 4. Synthesis of 4-methoxybenzaldehyde **8** by a two-phase oxidation reaction between 4-methoxybenzyl alcohol **7** in ethyl acetate (EtOAc) and aqueous NaClO without the use of PTC: (a) reaction schematic; HPLC chromatograms of two-phase oxidation reaction in (b) bulk phase and (c) HUN microdroplets after 3 min. Plots of $\ln(C_t/C_0)$ vs time deriving the pseudo first-order reaction rate constant to be (d) 1.1×10^{-6} s^{-1} in the "initial-rate region" of bulk phase and (e) 7.3×10^{-3} s^{-1} in HUN microdroplets.

Figures 4b and 4c show respectively the HPLC chromatograms of the two-phase reaction in bulk phase and HUN microdroplets after 3 min. In sharp contrast with that (0.1%) in bulk phase, a strikingly higher yield (75.4%) of product (4-methoxybenzaldehyde **8**) can be obtained by the HUN microdroplet reaction. The bulk reaction was also investigated for a longer reaction time, and we found that there were abundant byproducts (such as 4-chloroanisole and 3-chloro-4-methoxybenzaldehyde) in addition to the oxidation reaction product **8** in the two-phase reaction without the use of PTC in bulk phase (Figure S11). Gas chromatography mass spectrometry and nuclear magnetic resonance (NMR) enabled the identification of these byproducts (Figure S12 and S13). The bulk reaction was monitored by HPLC for 7 h, and Figure S14 presents the temporal peak area profiles of reactants and products. According to previous studies,[59, 60] the possible reaction pathway for the two-phase reaction in bulk phase is proposed to be as shown in Scheme S1. In the initial stage, reaction of 4-methoxybenzyl alcohol with NaClO resulted in 4-chloroanisole through ipso substitution in addition to the oxidation product (4-methoxybenzaldehyde), which is consistent with a previous report.[60] Then the chlorination reaction of the newly formed 4-methoxybenzaldehyde with NaClO generated 3-chloro-4-methoxybenzaldehyde.[59] After 7 h of bulk reaction, the yield of 4-methoxybenzaldehyde **8** was determined to be only 11.3% (owing to the formation of byproducts) by using a standard calibration curve of 4-methoxybenzaldehyde. These results also indicate that in addition to rate acceleration, highly selective synthesis of 4-methoxybenz-aldehyde **8** was facilitated by HUN

microdroplets. As noted in previous reports,[5, 20] the acceleration of reaction rate in microdroplets can be largely attributed to the accumulation of reactants on the surface of microdroplets. For this reaction, the concentrated NaClO on HUN microdroplets can also change the pH on the microdroplet surface. According to the previous report,[60] the byproduct, 4-chloroanisole, formed by ipso substitution of 4-methoxybenzyl alcohol with hypochlorite (ClO⁻) is strongly affected by pH. Thus, we speculate that the special pH microenvironment in HUN microdroplets inhibited the ipso substitution and at the same time, the production of another product, 3-chloro-4-methoxybenzaldehyde, was avoided by the short reaction time in HUN microdroplets.

In this two-phase reaction, the concentration of sodium hypochlorite (NaClO) was much higher than that of 4-methoxybenzyl alcohol **7.** Consequently, this reaction is presumed to proceed as a pseudo first-order reaction, which was confirmed by the kinetic analysis with reactant **7** at different initial concentrations (Figure S9). The reaction rates in bulk and HUN microdroplets were derived by plotting $\ln(C_t/C_0)$ of reactant **7** vs time, as shown in Figures 4d and 4e. The acceleration factor for this reaction in HUN microdroplets was determined to be 6536. In the HUN system, 93 mg product (4-methoxybenzaldehyde **8**) of the two-phase reaction with 68.4% yield was produced within 3 min (31 mg min⁻¹), which is a large advance for the scale-up of microdroplet reactions compared with that (1.2 mg min⁻¹)[16] obtained by a previous multiplexed ESI sprayer method (15 µL/min per spray tip).

Encouraged by these results, we further examined the applicability of this new method for a new reaction, i.e., the preparative synthesis of enaminone by the Eschemoser coupling reaction, which has not been examined previously by microdroplet reaction. Enaminones are important building blocks in organic synthesis and the Eschemoser coupling reaction has been extensively employed in the construction of enaminones.[61, 62] However, the coupling reaction often requires a long reaction time.[63-65]
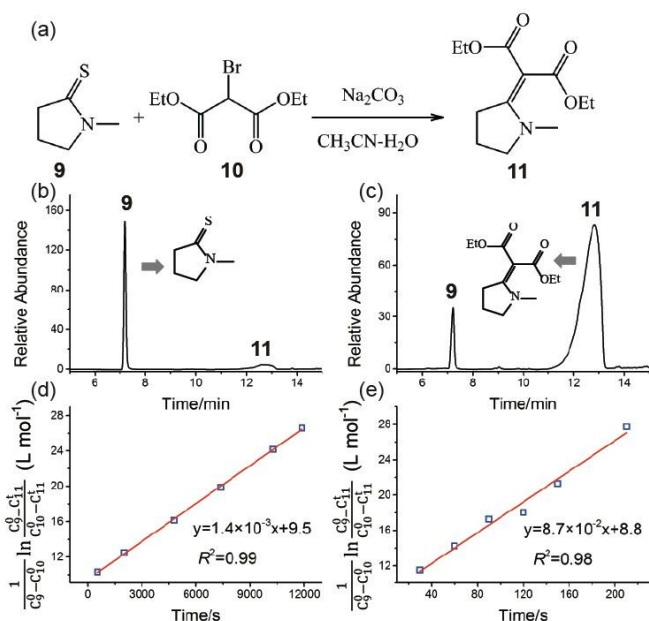
Chemical Science

Figure 5. The Eschenmoser coupling reaction of 1-methylpyrrolidine-2-thione **9** with diethyl bromomalonate **10** to form the enaminone product **11**: (a) reaction schematic; HPLC chromatograms of Eschenmoser coupling reaction in (b) bulk phase and (c) HUN microdroplets after 3.5 min. Plots of $1/(C_9^0 - C_{10}^0)\ln[(C_9^0 - C_{11}^t)/(C_{10}^0 - C_{11}^t)]$ vs time deriving the second-order reaction rate constant to be (d) 1.4×10^{-3} L mol^{-1} s^{-1} in the bulk phase and (e) 8.7×10^{-2} L mol^{-1} s^{-1} in HUN microdroplets.

Figure 5a shows the reaction schematic of the Eschemoser coupling reaction between 1-methylpyrrolidine-2-thione **9** and diethyl bromomalonate **10** to form the enaminone product **11**. The HPLC chromatograms of the Eschemoser coupling reaction in bulk phase and HUN microdroplets after 3.5 min were shown in Figures 5b and 5c, respectively. In comparison with the 3.5-min yield in bulk phase (6.2%), the 3.5-min yield (78%) obtained by the HUN microdroplet reaction is much higher. The initial concentration of diethyl bromomalonate **10** (C_{10}^0) in this experiment was 1.5 times higher than that of 1-methylpyrrolidine-2-thione **9** (C_9^0) and thus this reaction proceed as a second order reaction with reactants at different initial concentrations. The reaction rate constants in bulk phase (k_{bulk}) and HUN microdroplets (k_{HUN}) were calculated by plotting $1/(C_9^0 - C_{10}^0)\ln[(C_9^0 - C_{11}^t)/(C_{10}^0 - C_{11}^t)]$ vs reaction time (C_{11}^t represents the concentrations of product **11**) in Figures 5d and 5e. An acceleration factor for this reaction in HUN microdroplets was calculated to be 62. By using the HUN scale-up setup, 140 mg product was produced within 3.5 min with 67% yield (40 mg min^{-1}). Its ^{1}HNMR spectrum is provided after purification (Figure S16).

Conclusions

In summary, we have developed a new method for the scale-up of microdroplet reactions based on the HUN system. Four reactions including a base-catalyzed Claisen–Schmidt condensation, an oximation reaction, a two-phase reaction without the use of a phase transfer catalyst, and an Eschenmoser coupling reaction were examined. The rates of these reactions can be markedly accelerated in HUN microdroplets by one to three orders of magnitude higher than the corresponding bulk reactions. In addition we demonstrated that these reactions could be scaled up by an industrial nebulization plate with multiple nebulizers. By this means,

19-40 mg min^{-1} products were synthesized in HUN microdroplets. The above results indicate that microdroplet chemistry shows promise for the semi-preparative synthesis of many different compounds.

Experimental

For the Claisen-Schmidt condensation reaction, 50 mM 6-hydroxy-1-indanone, 50 mM benzaldehyde and 1.8 M KOH were mixed in equal volumes and methanol was the solvent. For the Oximation reaction, 50 mM benzophenone and 1 M hydroxylamine dissolved in 1 M NaOH were mixed in equal volumes and methanol was used as solvent. For the two-phase oxidation reaction, 200 mM 4-methoxybenzyl alcohol in EtOAc and aqueous NaClO (11-14%) were mixed at a volume ratio of 5:6. For the Eschenmoser coupling reaction, 87 mM 1-methylpyrrolidine-2-thione, 130 mM diethyl bromomalonate and 87 mM Na$_2$CO$_3$ were mixed and CH$_3$CN/H$_2$O (v:v=9:1) was used as the solvent.

Microdroplet reactions were conducted in nebulization cell with the temperature of heating tape set at 50 °C. For comparison, bulk reactions were conducted in a 50 °C water bath. Upon completion of the reaction, the products were collected and diluted for subsequent analysis by using a LTQ XL Orbitrap hybrid mass spectrometer (Thermo Fisher Scientific, Germany) or an Agilent 1260 high-performance liquid chromatography (HPLC) (Agilent, USA). The size of microdroplets in nebulization cell was measured by a laser diffractometer (Sympatec HELOS, Sympatec, Germany). Additional experimental details on each reaction system can be found in the Supporting Information (Sections S1 and S2). Preparative synthesis of the microdroplet reactions was facilitated by using an industrial nebulization plate with 10 ultrasonic nebulizers (A10D48-001, Dongguan RunYang Electronic Co., Ltd., China).

Conflicts of interest

There are no conflicts to declare.

Acknowledgements

Notes and references

1   1.   X. Yan, R. M. Bain and R. G. Cooks, *Angew. Chem. Int Ed.*, 2016, **55**, 12960-12972.

2   2.   M. Girod, E. Moyano, D. I. Campbell and R. G. Cooks, *Chem. Sci.*, 2011, **2**, 501-510.

Chemical Science Accepted Manuscript

3. 3. T. Muller, A. Badu-Tawiah and R. G. Cooks, *Angew. Chem. Int Ed.*, 2012, **51**, 11832-11835.

4. 4. R. M. Bain, C. J. Pulliam and R. G. Cooks, *Chem. Sci.*, 2015, **6**, 397-401.

5. 5. Z. Zhou, X. Yan, Y.-H. Lai and R. N. Zare, *J. Phys. Chem. Lett.*, 2018.

6. 6. N. Sahota, D. I. AbuSalim, M. L. Wang, C. J. Brown, Z. Zhang, T. J. El-Baba, S. Cook and D. E. Clemmer, *Chem. Sci.*, 2019.

7. 7. T. Kenderdine, Z. Xia, E. R. Williams and D. Fabris, *Anal. Chem.*, 2018, **90**, 13541-13548.

8. 8. D. N. Mortensen and E. R. Williams, *Anal. Chem.*, 2014, **87**, 1281-1287.

9. 9. D. N. Mortensen and E. R. Williams, *J. Am. Chem. Soc.*, 2016, **138**, 3453-3460.

10. 10. G. I. Ioannou, T. Montagnon, D. Kalaitzakis, S. A. Pergantis and G. Vassilikogiannakis, *Org. Biomol. Chem.*, 2017, **15**, 10151-10155.

11. 11. G. I. Ioannou, T. Montagnon, D. Kalaitzakis, S. A. Pergantis and G. Vassilikogiannakis, *ChemPhotoChem*, 2018, **2**, 860-864.

12. 12. S. Banerjee and R. N. Zare, *Angew. Chem. Int Ed.*, 2015, **54**, 14795-14799.

13. 13. J. K. Lee, Samuel Kim, Hong Gil Nam, Richard N. Zare., *Proc. Natl. Acad. Sci. USA*, 2015, **201503689**.

14. 14. J. K. Lee, S. Banerjee, H. G. Nam and R. N. Zare, *Q. Rev. Biophys.*, 2015, **48**, 437-444.

15. 15. E. T. Jansson, Y. H. Lai, J. G. Santiago and R. N. Zare, *J. Am. Chem. Soc.*, 2017, **139**, 6851-6854.

16. 16. X. Yan, H. Cheng and R. N. Zare, *Angew. Chem. Int Ed.*, 2017, **129**, 3616-3619.

17. 17. B. Sharma, Y. Takamura, T. Shimoda and M. Biyani, *Sci. Rep.*, 2016, **6**, 26257.

18. 18. A. Fallah-Araghi, K. Meguellati, J. C. Baret, A. El Harrak, T. Mangeat, M. Karplus, S. Ladame, C. M. Marques and A. D. Griffiths, *Phys. Rev. Lett.*, 2014, **112**, 028301.

19. 19. M. Guardingo, F. Busqué and D. Ruiz-Molina, *Chem. Commun.*, 2016, **52**, 11617-11626.

20. 20. S. Mondal, S. Acharya, R. Biswas, B. Bagchi and R. N. Zare, *J. Chem. Phys.*, 2018, **148**, 244704.

21. 21. H. Wei, E. P. Vejerano, W. Leng, Q. Huang, M. R. Willner, L. C. Marr and P. J. Vikesland, *Proc. Natl. Acad. Sci. USA*, 2018, **115**, 7272-7277.

22. 22. R. M. Bain, C. J. Pulliam, F. Thery and R. G. Cooks, *Angew. Chem. Int Ed.*, 2016, **55**, 10478-10482.

23. 23. Y. Li, X. Yan and R. G. Cooks, *Angew. Chem. Int Ed.*, 2016, **55**, 3433-3437.

24. 24. Z. Wei, M. Wleklinski, C. Ferreira and R. G. Cooks, *Angew. Chem. Int Ed.*, 2017, **129**, 9514-9518.

25. 25. K. Holmberg, *Curr. Opin. Colloid In*, 2003, **8**, 187-196.

26. 26. K. Holmberg, *Adv. Colloid Interfac.*, 1994, **51**, 137-174.

27. 27. L. García-Río, J. R. Leis, J. C. Mejuto and M. Pérez-Lorenzo, *Pure Appl. Chem.*, 2007, **79**, 1111-1123.

28. 28. H. Song, D. L. Chen and R. F. Ismagilov, *Angew. Chem. Int. Edit.*, 2006, **45**, 7336-7356.

29. 29. J. Wang, G. Sui, V. P. Mocharla, R. J. Lin, M. E. Phelps, H. C. Kolb and H. R. Tseng, *Angew. Chem. Int. Edit.*, 2006, **45**, 5276-5281.

30. 30. J. J. Agresti, E. Antipov, A. R. Abate, K. Ahn, A. C. Rowat, J.-C. Baret, M. Marquez, A. M. Klibanov, A. D. Griffiths and D. A. Weitz, *Proc. Natl. Acad. Sci. USA*, 2010, **107**, 4004-4009.

31. 31. K. Churski, P. Korczyk and P. Garstecki, *Lab Chip*, 2010, **10**, 816-818.

32. 32. A. J. Demello, *Nature*, 2006, **442**, 394.

33. 33. K. Geyer, T. Gustafsson and P. H. Seeberger, *Synlett*, 2009, **2009**, 2382-2391.

34. 34. S. Taghavi-Moghadam, A. Kleemann and G. Golbig, *Org. Process Res. Dev.*, 2001, **5**, 652-658.

35. 35. D. R. Acke and C. V. Stevens, *Org. Process Res. Dev.*, 2006, **10**, 417-422.

36. 36. X. Zhang, S. Stefanick and F. J. Villani, *Org. Process Res. Dev.*, 2004, **8**, 455-460.

37. 37. I. Nam, J. K. Lee, H. G. Nam and R. N. Zare, *Proc. Natl. Acad. Sci. USA*, 2017, **114**, 12396-12400.

38. 38. D. Gao, F. Jin, X. Yan and R. N. Zare, *Chem.–Eur. J.*, 2018.

39. 39. Y. H. Lai, S. Sathyamoorthi, R. M. Bain and R. N. Zare, *J. Am. Soc. Mass Spectrom.*, 2018, **29**, 1036-1043.

40. 40. I. Nam, H. G. Nam and R. N. Zare, *Proc. Natl. Acad. Sci. USA*, 2018, **115**, 36-40.

41. 41. R. W. Wood and A. L. Loomis, *Philos. Mag.*, 1927, **4**, 417-436.

42. 42. M. A. Tarr, G. Zhu, R.F. Browner, *Anal. Chem.*, 1993, **65**, 1689-1695.

43. 43. M. A. M. da Silva, V.L.A Frescura, A.J. Curtius, *Spectrochim. Acta. B* 2000, **55**, 803-813.

44. 44. J. Shiea, D.Y. Chang, C.H. Lin, S.J. Jiang, *Anal. Chem.*, 2001, **73**, 4983-4987.

45. 45. D.-Y. Chang, C.-C. Lee and J. Shiea, *Anal. Chem.*, 2002, **74**, 2465-2469.

46. 46. L. Zhu, G. Gamez, H. Chen, K. Chingin, R. Zenobi, *Chem. Commun.*, 2009, DOI: 10.1039/b818541g, 559-561.

47. 47. C. Liu, Y. Zhu, Z. Zhou, J. Yang, F. Qi and Y. Pan, *Anal. Chim. Acta.*, 2015, **891**, 203-210.

48. 48. C. Liu, J. Yang, J. Wang, Y. Hu, W. Zhao, Z. Zhou, F. Qi and Y. Pan, *J. Am. Soc. Mass Spectrom.*, 2016, **27**, 1597-1605.

49. 49. Y. T. Didenko and K. S. Suslick, *J. Am. Chem. Soc.*, 2005, **127**, 12196-12197.

50. 50. S. E. Skrabalak and K. S. Suslick, *J. Am. Chem. Soc.*, 2006, **128**, 12642-12643.

51. 51. J. H. Bang and K. S. Suslick, *Adv. Mater.*, 2010, **22**, 1039-1059.

52. 52. E. A. Crawford, C. Esen and D. A. Volmer, *Anal. Chem.*, 2016, **88**, 8396-8403.

53. 53. R. M. Bain, C. J. Pulliam, X. Yan, K. F. Moore, T. Müller and R. G. Cooks, *J. Chem. Educ.*, 2014, **91**, 1985-1989.

Chemical Science

ARTICLE

Chemical Science Accepted Manuscript

54   54.   W. Zhang, H. Cheng and J. Liu, *ACS Sustain. Chem. Eng.*, 2018, **6**, 8125-8129.

55   55.   X. Yan, Y.-H. Lai and R. N. Zare, *Chem. Sci.*, 2018, **9**, 5207-5211.

56   56.   J. K. Lee, D. Samanta, H. G. Nam and R. N. Zare, *J. Am. Chem. Soc*, 2019, **141**, 10585-10589.

57   57.   L. Guy Donaruma and W. Z. Heldt, *Org. React.*, 2004, **11**, 1-156.

58   58.   W. Zhang, S. Yang, Q. Lin, H. Cheng and J. Liu, *J. Org. Chem.*, 2018, **84**, 851-859.

59   59.   A. T. Lebedev, G. M. Shaydullina, N. A. Sinikova and N. V. Harchevnikova, *Water Res.*, 2004, **38**, 3713-3718.

60   60.   H. V. Carrillo, A. Y. Rodriguez, R. G. Landolt and W. H. Hendrickson, *Synlett*, 2011, **22**, 2069-2071.

61   61.   Shiosaki, K. In Comprehensive Organic Synthesis; Trost, B. M., Flemming, I., Eds.; Pergamon Press: Oxford, U.K., 1991; Vol. 2, Chapter 3.7, p 865.

62   62.   N. D. Koduri, H. Scott, B. Hileman, J. D. Cox, M. Coffin, L. Glicksberg and S. R. Hussaini, *Org. Lett.*, 2011, **14**, 440-443.

63   63.   S. R. Hussaini and M. G. Moloney, *Org. Biomol. Chem.*, 2006, **4**, 2600-2615.

64   64.   J. A. Campbell and H. Rapoport, *J. Org. Chem.*, 1996, **61**, 6313-6325.

65   65.   N. D. Koduri, B. Hileman, J. D. Cox, H. Scott, P. Hoang, A. Robbins, K. Bowers, L. Tsebaot, K. Miao and M. Castaneda, *RSC Adv.*, 2013, **3**, 181-188.

66